Journal of Catalysis **193,** 338–347 (2000)
doi:10.1006/jcat.2000.2887, available online at http://www.idealibrary.com on IDEAL®

The Dynamics of Oxygen Storage in Ceria–Zirconia Model Catalysts Measured by CO Oxidation under Stationary and Cycling Feedstream Compositions

Marta Boaro, Carla de Leitenburg, Giuliano Dolcetti, and Alessandro Trovarelli

Dipartimento di Scienze e Tecnologie Chimiche, Università di Udine, via Cotonificio 108, 33100 Udine, Italy
E-mail: trovarelli@dstc.uniud.it

Received February 15, 2000; revised April 6, 2000; accepted April 7, 2000

Measurements were made of the dynamics of CO oxidation over a series of fresh and aged CeO_2–ZrO_2 catalysts of different composition. In order to evaluate the varying contributions to oxygen storage/release capacity, we carried out the reaction under transient "anaerobic environment" (in both pulse and cycling mode) and steady-state conditions. The presence of ZrO_2 was of little or no benefit to stoichiometric CO oxidation carried out under stationary conditions. Under these conditions, catalytic activity is strongly dependent on surface area and on the number of exposed cerium atoms. The highest performance level is achieved with pure ceria. The beneficial effect of CeO_2–ZrO_2 mixed oxides on catalytic performance was observed when CO oxidation was carried out in transient pulse mode or under cycling feedstream composition. In this case, catalysts having the composition $Ce_xZr_{1-x}O_2$ with $0.5 < x < 0.8$ show an increased catalytic effectiveness correlated to their oxygen storage capacity and redox activity. The promotional effect of ZrO_2 was much more evident after severe aging. The decrease in oxygen storage activity with pure CeO_2 was higher than that observed for ceria-zirconia and was mainly correlated to the drop in surface area. In contrast with ceria, the low-temperature activity of CeO_2–ZrO_2 solid solutions for CO oxidation under anaerobic conditions was positively dependent on the degree of reduction of the material. A quantitative estimate of the contribution of bulk diffusion to the overall performance was carried out by calculating the O^{2-} diffusion coefficient. These values were calculated from conductivity measurements using the Nernst–Einstein relation. It is shown that, in the temperature range investigated, bulk diffusion was approximately two orders of magnitude higher for ceria–zirconia than for ceria and may have been responsible for the enhancement of CO conversion observed with respect to ceria–zirconia-based catalysts.

Key Words: **ceria; CeO_2; ceria–zirconia; CeO_2–ZrO_2; oxygen storage capacity; three-way catalysts; auto-exhaust catalysts; CO oxidation; redox behavior; oxygen diffusion coefficients.**

INTRODUCTION

Ceria–zirconia is one of the main components of the current new generation of three-way catalysts (TWC) for the treatment of noxious pollutants from car exhaust (1). It has gradually replaced pure cerium oxide (CeO_2), whose characteristics were inadequate to sustain the high degree of conversion and the thermal resistance required for catalytic converters to comply with increasingly severe regulations regarding emissions of CO, NO_x, and hydrocarbons (HCs). The main features which contribute to the success of these components are: (i) higher thermal resistance, compared to conventional ZrO_2-free TWCs (2); (ii) a higher reduction efficiency of redox couple Ce^{4+}/Ce^{3+} (3, 4); (iii) the possibility of preventing the undesired formation during reaction of $CeAlO_3$, which contributes to the deactivation of the catalyst (1); and (iv) excellent oxygen storage/release capacity (OSC), compared to pure ceria (5–9).

Oxygen storage capacity is related to the ability of the catalyst to sustain deviation from stoichiometric composition in the feedstream while maintaining a high degree of conversion, to release oxygen during oscillations in the rich composition side (enhancing CO and HC conversion), and to take up oxygen in the lean portion of oscillation (enhancing NO_x conversion to N_2) (10). These oscillations occur with a frequency of approximately 1 Hz. Nevertheless, during driving cycles, and especially on acceleration and deceleration, strong deviations from this value can occur, leaving the catalyst under lean/rich conditions for a longer time. This implies that the mechanism by which oxygen is stored and released must be fast, in order to be able to provide/remove oxygen in the time scale of oscillations, but it must also be capable of sustaining conversion during longer excursions on the rich and lean side, respectively. In this regard, it is important to differentiate between total OSC and dynamic, or fast, OSC. The former is related to the total degree of reduction at a given temperature whereas the second is a measure of the amount of oxygen transferred in a transient regime which best simulates the oscillations which the exhaust gas may undergo. It therefore represents the oxygen which is kinetically available during the fast transitions between reduction and oxidation environments. It is a more important value than the total O_2 uptake since a large uptake is of no consequence unless it is reversible

0021-9517/00 $35.00

on the time scale of exhaust fluctuations. The actual importance of this process during dynamic operations is thus determined first by the rate of variation in the oxygen content and second by the oxygen capacity of the material, i.e., its reducibility.

Several research groups have recently investigated the reduction properties of ceria–zirconia catalysts, which are related to their oxygen-storage capacity (3–14). It has been found that the introduction of the smaller Zr cation into the cubic lattice of ceria strongly promotes the reduction of Ce^{4+} to Ce^{3+}, especially at low temperature. Moreover, reduction properties seem to be rather independent of surface area, in contrast to what happens with pure ceria, where the first 20–30% reduction is strongly influenced by morphology and surface area (15). Composition (Ce/Zr ratio) can also significantly change reduction behavior. This is a consequence of the change in the concentration of active redox element Ce^{4+} and of different structural features in the solid solutions. Results seem to indicate that cubic $Ce_xZr_{1-x}O_2$ ($0.5 < x < 0.8$) has a superior performance in terms of overall reduction and total oxygen storage (1, 16). This behavior is consistent with a structural modification of the fluorite cell induced by the introduction of zirconia, which brings about a higher lability in some oxygen ions, thus enhancing their diffusion rate (3, 5). Recently, however, other interpretations have been put forward. Hori *et al.* (7) suggested that surface processes, rather than migration of oxygen in the bulk, were limiting the reduction process rate. Although both textural and structural factors certainly govern the redox behavior of these mixed oxides, there are many aspects, especially of high surface area systems, that still deserve further investigation.

In the present work, we studied CO oxidation over a series of CeO_2–ZrO_2 mixed oxides having different composition. To evaluate the contribution of true oxygen storage to overall CO oxidation activity, we carried out the reaction under different experimental conditions using catalysts with different compositions. CO oxidation activity measurements under stationary steady-state conditions should indicate the catalyst performance when both reagents (CO and O_2) are fed simultaneously, with the oxygen storage/release contribution kept to a minimum. In contrast, CO oxidation under pulsed conditions is a measure of catalyst oxidation/reduction ability, which is more related to the total OSC, or to values characteristic of significant deviation from stoichiometry. The oxidation of CO carried out under oscillating feedstream conditions carries contributions both from CO oxidation with gas-phase oxygen and from redox reaction from the support. This gives a more precise indication of the efficiency of the OSC for these catalysts under conditions of rapid variation in the stoichiometric composition, which are closer to those found in catalytic converters.

EXPERIMENTAL

Characterization of Materials

Fresh, high-surface-area samples of ceria and ceria–zirconia were generously provided by Rhodia, and their characteristics are summarized in Table 1. The structural and textural details of these supports have been the subject of recent investigations and are available in the literature (17, 18). Samples of intermediate (MSA) and low (LSA) surface area were obtained by calcination in the temperature range $773\ K < T < 1173\ K$ for 3–5 h.

For catalytic measurements, the supports were previously treated under air flow (60 N ml/min) from room temperature to 773 K at a rate of 10 K per minute and kept under an oxidizing atmosphere for 1 h.

The effects of redox aging were investigated for $Ce_{0.50}Zr_{0.50}O_2$ and CeO_2. The samples were prepared *in situ* by heating under H_2 to 1273 K (50 N ml/min at 10 K/min) and keeping at this temperature for different times in order to reach similar surface area with both compositions. Thus ceria was treated for 10 min while a 2-h treatment was needed for $Ce_{0.50}Zr_{0.50}O_2$ under identical conditions. After this treatment, the samples were cooled to 773 K and reoxidized for 1 h before catalytic measurements. Final surface areas were 5 m^2/g for CeO_2 and 11 m^2/g for $Ce_{0.50}Zr_{0.50}O_2$.

Surface-area measurements were carried out with a Sorptomatic 1900 instrument (Carlo Erba) using the BET method.

Catalytic Activity

CO-oxidation experiments were carried out with three different reactor configurations in stationary, pulse, and cycling modes. Details of the systems are given below.

Steady-state reactor working under stationary and cycling feedstream conditions. The gas manifold consists of five mass flow controllers which supply reaction and treatment gases to the reactor. Downstream of the flow controller, a three-way valve system allows the reactor to be operated under stationary or cycling feedstream conditions. Under stationary conditions, a mixture of CO (4% in He) and O_2 (2% in He) was fed to the reactor at a total flow of

TABLE 1

Characteristics of Samples Used in This Study

Samples	Composition	Surface area (m^2/g)		
		Fresh HSA	MSA	LSA
CZ100	CeO_2	97	59	10
CZ80	$Ce_{0.80}Zr_{0.2}O_2$	108	34	12
CZ68	$Ce_{0.68}Zr_{0.32}O_2$	99	41	12
CZ50	$Ce_{0.5}Zr_{0.5}O_2$	105	68	16
CZ15	$Ce_{0.15}Zr_{0.85}O_2$	92	54	18

0.1 N l/min. The reactor consists of a 6-mm o.d. by 4-mm i.d. by 440–mm-long quartz tube vertically mounted in a single-zone furnace, which allows the catalyst temperature to be maintained between 298 and 1273 K. A chromel–alumel thermocouple enters the top of reactor and measures the catalyst-inlet temperature (i.e., reaction temperature). The powdered catalyst (0.01–0.1 g) is loaded after being mixed with an equal amount of quartz beads ($200 < \emptyset < 350$ μm) and is located at the center of furnace, supported in the reactor on a quartz-wool bed.

The cycling operation was effected using a system of five electronically driven solenoid valves. A software handle switched the valves at a desired frequency according to predefined sequences. This enabled the reactor to be fed with a gaseous mixture whose composition cycle lies between defined values. A vent pressure regulator was used to maintain the system outlet flow at a constant level to control flow into the reactor and prevent pressure bursts. At the reactor outlet, the gas flow passed through a mixing zone and the time-averaged concentration of the outlet mixture was analyzed by a gas chromatograph. The reactor was loaded with 0.01–0.1 g of catalyst and was fed at a total flow of 0.12 N l/min. The composition was cycled alternately between CO (4%) and O_2 (2%) with a short cycle, consisting of 1 s in CO and 1 s in O_2 with a 2 s pulse of He in between. This was done in order to ensure flushing of gas species between pulsing, thus limiting direct reaction between CO and O_2, which could otherwise have mixed before reaching the reactor. No mixing of CO and oxygen before contact with the catalyst was observed, as verified by a mass spectrometer located before the catalyst bed. A short-system response time with limited pulse dilution was achieved by using miniature fast-response solenoid valves and 1/16-in o.d. stainless steel tubing for connections upstream of the reactor. A dilution volume (0.2 N l) was placed after the reactor to analyze the time-averaged concentration of outlet gases. Proper mixing of the gases was checked through the empty reactor for flow rates ranging from 40 to 120 N ml/min by comparing the composition of the mixture with that calculated for the gases if they had been fed simultaneously into the reactor. The results of this test indicated that complete mixing was achieved before analysis. We therefore used the time-averaged $CO_2/(CO + CO_2)$ ratio as a measure of the oxygen storage capacity of the samples.

Pulse reactor. Other more conventional OSC measurements were carried out in a pulse reactor, according to a previously reported procedure (19). The catalyst (0.01 g) was placed on a bed of quartz in a stainless steel tubular microreactor ($\phi = 1/4$ in, $L = 150$ mm) and was kept at the desired temperature (673 K) using a couple of heating resistances. Pulses of reacting gases were injected into the carrier gas (He, 30 N ml/min) through a four-way valve connected to a gas-sampling loop of 0.5 ml. Five O_2 pulses (2% in He) injected every 2 min were followed by a pulse of CO (4% in He). The OSC of the catalyst was measured as μmol of CO_2 produced *per gram* of catalyst. A gas chromatograph equipped with a TCD detector was used to determine the O_2, CO, and CO_2 contents of the exhaust gas.

RESULTS AND DISCUSSION

The effect of temperature on CO conversion measured for ceria and ceria–zirconia under stationary and cycling conditions is reported in Figs. 1 and 2, respectively. As can be seen in both cases, a typical "smooth" light-off behavior is observed and conversion increases slightly with temperature. The shape of the curves shows that conversion is negligible at low temperatures, increases at around 500–600 K, and approaches total conversion for the most active samples at $T > 750$–800 K. Although the absolute value of overall conversion collected under the two experimental modes cannot be directly compared in a quantitative manner, the data deserve some qualitative comments. The overall conversion is generally higher when measured under oscillating conditions in the range of temperatures examined. This is true for all samples except for pure CeO_2 and CZ15 (and at high temperatures for CZ80), where conversion under steady-state conditions is higher than that measured in oscillating mode. It seems that cerium is responsible for the activity of the mixed oxides under stationary conditions while the presence of zirconium significantly contributes to the activity changes observed in oscillating mode. This situation closely resembles that observed by Gonzalez-Velasco *et al.* (20), who found that, for CO oxidation under stationary conditions, cerium is expected to be responsible for the activity of the mixed oxides. The effect of composition is

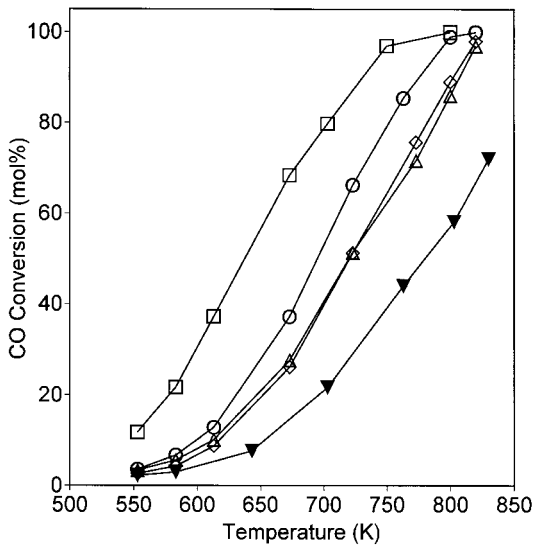

FIG. 1. CO conversion under stationary conditions versus temperature for various Ce/Zr mixed oxides. Reaction conditions: total flow 0.10 N l/min, $P(CO) = 15.2$ Torr, $P(O_2) = 7.6$ Torr, balance He; cat. wt. 10 mg. (□) CZ100, (○) CZ80, (△) CZ68, (◇) CZ50, (▼) CZ15.

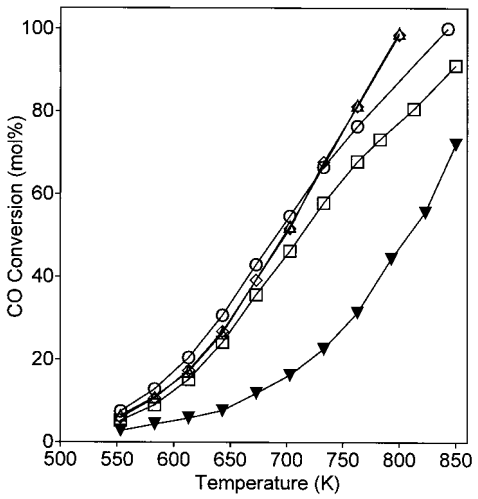

FIG. 2. CO conversion under cycling feedstream conditions versus temperature for various Ce/Zr mixed oxides. Reaction conditions: total flow 0.12 N l/min, cycling frequency ca. 1 Hz, $P(CO) = 30.4$ Torr, $P(O_2) = 15.2$ Torr, balance He, cat. wt. 10 mg. (□) CZ100, (○) CZ80, (△) CZ68, (◇) CZ50, (▼) CZ15.

better evidenced when reaction-rate values are calculated under the two different regimes (Fig. 3). In one case, the rate is almost proportional to the amount of ceria whereas, in the other situation, the rate reaches a maximum when CeO_2 content is within the range 50–80 mol%. For that reason, since the surface area of all samples is similar (see Table 1), it seems that the rate under stationary conditions is determined by the number of exposed redox sites (Ce^{4+}). In contrast, under oscillating conditions, there is an optimum composition where a maximum of reaction rates is found. This indicates that purely surface factors cannot readily explain CO oxidation behavior in fast oscillating mode and that CO oxidation paths in the presence of ZrO_2 probably include a number of contributions.

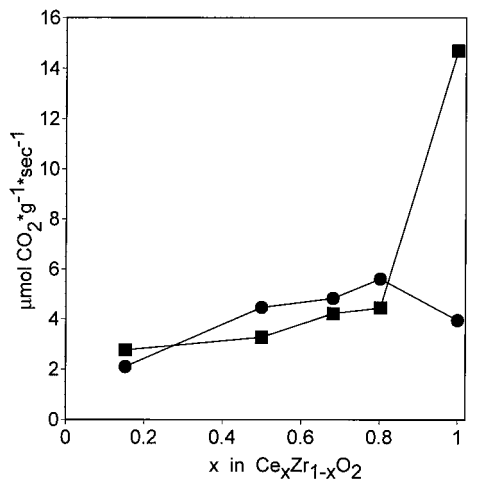

FIG. 3. Reaction rate per gram of catalyst under cycling (●) and stationary (■) conditions for various Ce/Zr compositions ($T = 533$ K).

CO oxidation may follow various reaction mechanisms, according to experimental conditions and catalyst composition. CO oxidation on pure ceria occurs according to a Mars van Krevelen redox-type mechanism (15), in which CeO_2 is alternately reduced by CO and oxidized by gas-phase oxygen. Under these conditions, if oxygen is present in the gas phase, it will soon reoxidize the support and the surface site will be mainly involved in the process. If oxygen is not present, CO oxidation will depend first on surface oxygens of ceria and then, when these are consumed, on the availability of bulk oxygens. Under these conditions, the reaction mechanism is therefore connected to the intrinsic ability of the oxide to store and release oxygen, provided that surface steps are faster than bulk oxygen diffusion and migration.

We carried out CO oxidation measurements on the two supports under totally anaerobic conditions in a pulse reactor to discriminate between the role of bulk oxygen migration and surface reactivity in the oxygen storage of ceria and ceria–zirconia. In this case, conversion of CO to CO_2 is a measure of the ability of the catalyst to donate its oxygen. Since conversion occurs in the total absence of gas-phase oxygen, it may be indicative of the performance of the catalyst under conditions of substantial deviation from stoichiometry. Figure 4 shows a typical pulse-oxidation experiment conducted on CZ80 at 673 K. The oxygen released per pulse was measured in terms of micromoles of CO_2 per gram of catalyst. In these experiments, the amount of CO in one pulse was sufficient to reduce CeO_2

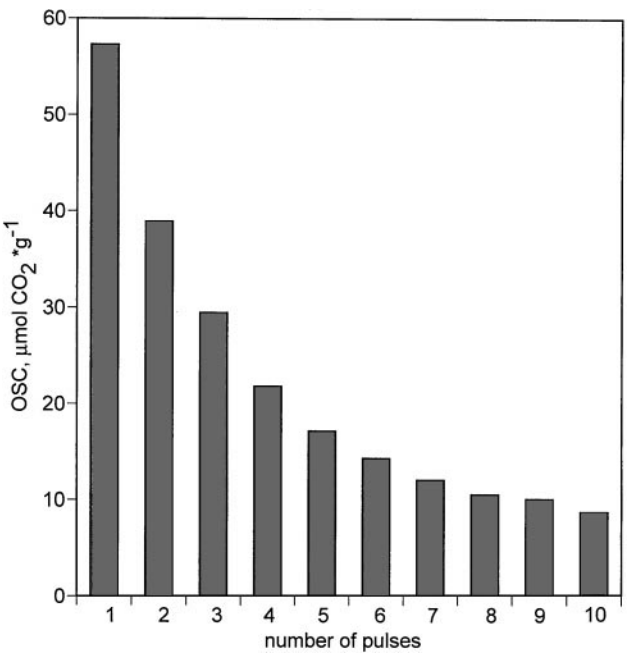

FIG. 4. A representative experiment of CO oxidation measured under pulse conditions in the absence of gaseous oxygen over CZ80. For conditions see text.

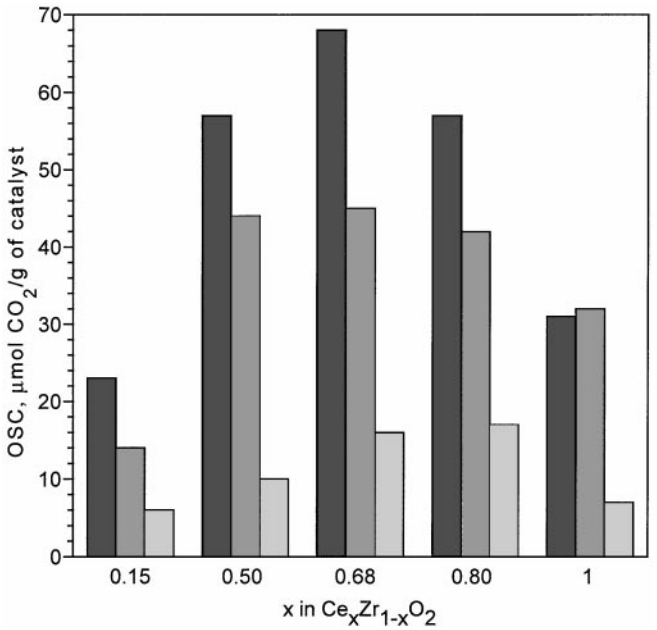

FIG. 5. Oxygen-storage capacity measured under pulse conditions for various Ce/Zr mixed oxides. Values measured after first pulse. Left bar, high-surface-area materials; middle bar, MSA; right bar, LSA.

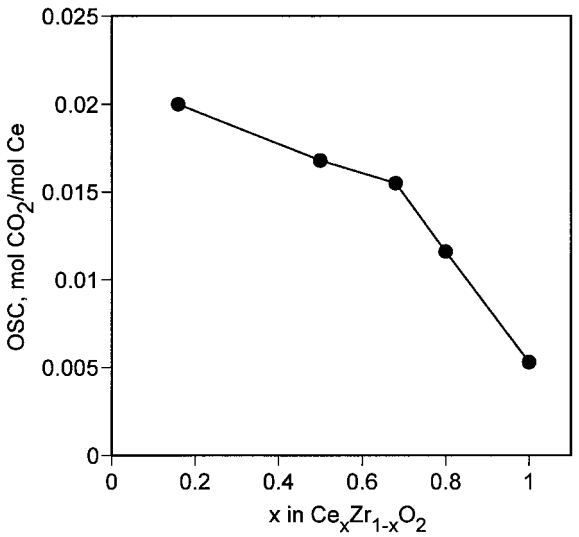

FIG. 6. Oxygen-storage capacity per cerium atom vs composition. Values measured after first pulse.

to approximately $CeO_{1.97}$. However, in all cases, CO conversion was less than 50% and total CO consumption was not a limiting factor in the reaction. Conversion per pulse decreases rapidly in the first five pulses (from ca. 50% to 15%) and then slowly when conversion is less than 10%. The results of total OSC are reported in Fig. 5 for all samples investigated. For each composition, three samples with different surface area were used. The best overall behavior was found for solid solutions with an intermediate composition ($Ce_xZr_{1-x}O_2$ with $0.5 \leq x \leq 0.8$). This result is in agreement with previous studies which investigated transient CO oxidation in similar samples (8). The difference in total CO consumption is due to the higher space velocity used in our investigation. Similar results were also obtained recently by Madier *et al.*, who investigated exchange of oxygen under similar conditions (21). A maximum at a different composition ($Ce_xZr_{1-x}O_2$ with $x = 0.75$) was found for transient CO oxidation at 873 K by Hori *et al.* (7). This maximum was shown to be sensitive to sample preparation and aging treatment, shifting to lower x values as aging temperatures increased. Other results based on the total reduction operated by H_2 instead of CO gave qualitatively similar behaviors (1), although the effect of preparation can substantially shift the maximum toward different compositions (6).

If the results are reported to highlight CO reacted per cerium content, the highest activity for fresh samples is at a lower cerium composition (Fig. 6). This may point to an enhanced Ce^{4+} reducibility for a $Ce_{0.15}Zr_{0.85}O_2$ system. However, a substantial amount of cerium is required for an efficient oxygen-storage capability, so an optimum balance must be found between the increased Ce reducibility and the concentration of ceria in the mixed oxides. This also explains why the conversion of CZ15 under oscillating mode is slightly lower than that observed under stationary conditions.

The participation of bulk oxygen in the process is evidenced in Fig. 7, which shows the amount of oxygen taken in every CO pulse (normalized to the number of oxygens initially available on the surface). This was calculated on the basis of one available surface oxygen out of four,

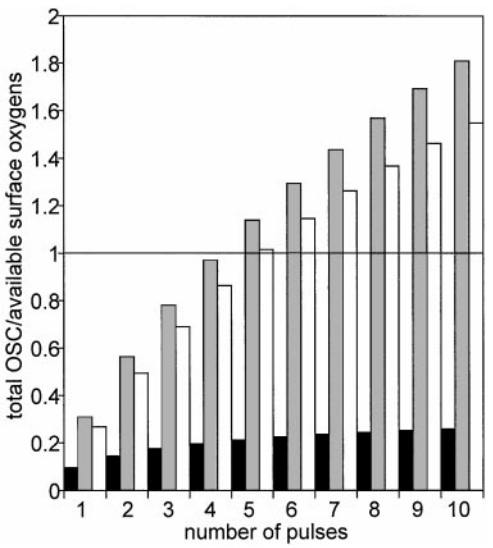

FIG. 7. Oxygen released (normalized to number of initially available surface oxygens) against pulse number for MSA samples: black bar, CZ100; gray bar, CZ15; white bar, CZ80.

corresponding to the reduction of Ce^{4+} to Ce^{3+}, and considering a cubic crystal of ceria with an interlayer distance of 0.541 nm with preferential exposure of (111), (110), and (100) surfaces. For ceria–zirconia, lattice constants were derived from the literature (3), and the number of available oxygens were calculated on the basis of composition ($0.25 * \text{total number of surface oxygen} * x$), assuming that there was no surface enrichment of Ce and Zr, considering that Zr atoms do not participate to the storage process and that (111), (110), and (100) surfaces are equally distributed on the surface. This approach, although not fully accurate for a model, gives a reasonable estimate of surface oxygens and has already been used for this purpose (21). For mixed oxides, it is shown that the quantity of surface oxygen was totally depleted after approximately five pulses and bulk oxygen was utilized for oxidation. With CeO_2, only part of the available surface oxygen was utilized. This agrees well with the known tendency of high-surface-area ceria to be reduced only on the surface or in the near-surface region in this temperature range (22, 23). Formation of surface vacancies is a much more favored process than the extraction of oxygen from the bulk (24–26). For ceria–zirconia, reduction studies indicate that the difference is less marked, with surface and bulk reduction occurring almost simultaneously (1, 3–6).

In general, the reduction of an oxide causes the formation of surface vacancies, which then migrate into the bulk. The rate-determining step can be either the formation of surface vacancies or their migration into the bulk. We measured the oxygen-storage and release properties of ceria and ceria–zirconia as a function of the degree of reduction with the specific intention of discriminating between the effects of surface (i.e., surface-active cerium atoms) and bulk (i.e., bulk transport of oxygen) phenomena. Figure 8 shows the oxygen storage capacity of different samples plotted against the degree of reduction. By measuring OSC at different reduction degrees, two situations arise: one is the decrease in the surface Ce^{4+} ions available for reduction, which limits the number of surface redox sites; the other is the increase in oxygen diffusion due to the greater number of oxygen vacancies. Diffusion of oxygen in ceria occurs through a classic hopping mechanism by means of vacancies, and diffusion coefficients depend positively on the degree of reduction (27). Thus, if diffusion controls OSC, oxygen released on the surface would be expected to increase as the material is progressively reduced. In contrast, reduction progressively empties the surface of active Ce^{4+} sites, which would limit the oxygen available for reduction. If we normalize OSC to the total number of surface-active sites available after each pulse, we can highlight the effect of diffusion by looking at the slope of the OSC vs degree of reduction curve. We see that the slope changes from negative to positive as x in $Ce_xZr_{1-x}O_2$ goes from 1 to 0.15. This indicates that pure CeO_2 (or mixed-oxide compositions with $x > 0.8$) exchanges less oxygen as more vacancies are created, demonstrating that in this case it is the generation of a new surface vacancy, and not diffusion of oxygen, that limits OSC and that bulk oxygen is not involved in the process. On the other hand, $Ce_xZr_{1-x}O_2$ mixed oxides with a composition of $x < 0.8$ show similar, or even enhanced, released oxygen as the material is progressively reduced and more vacancies are formed. An increase in oxygen storage as the number of surface redox sites is depleted can be explained only by an increase of oxygen diffusion, suggesting that oxygen-ion diffusion is involved in the reduction process, at least under these process conditions.

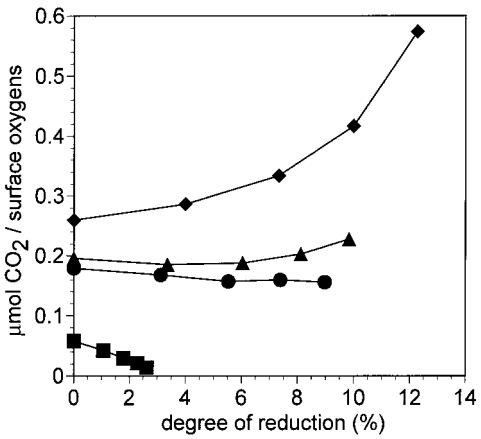

FIG. 8. CO oxidation under pulse conditions: CO_2 formation (normalized to number of surface oxygens available after each pulse) as a function of degree of reduction. (■) CZ100, (●) CZ68, (▲) CZ50, (◆) CZ15.

This result corroborates previous findings by Fornasiero *et al.*, who indicated that enhanced bulk oxygen diffusion may be responsible for the higher reducibility and the higher oxygen uptake observed in ceria–zirconia solid solutions (3, 28). In contrast, Hori *et al.* recently hypothesized that the rate-determining step in CO oxidation under anaerobic conditions is the creation of a new vacancy and not diffusion of O^{2-} in the lattice (7, 29). The origin of this discrepancy may be due to the different range of temperatures employed in the two studies as outlined by the authors. Moreover, Hori *et al.* calculated the flux of oxygen from the bulk to the surface, which was reported to be several orders of magnitude higher than the experimentally measured reaction rate. However, when estimating the diffusion rate of O^{2-} at temperature of 873 K, these authors extrapolated the values reported for pure ceria by Steele and Floyd (30), which are valid only in the temperature range $1123\ \text{K} < T < 1423\ \text{K}$. This probably gives an over-generous estimate of the oxygen diffusion coefficient in the lower temperature range (activation energy is not constant), which could lead to an over-estimation of the migration rate of O^{2-} in the system.

As far as we know, direct measurements of bulk diffusion coefficients for these materials, especially for ceria-rich compositions, have not been reported in the literature, while only a few data exist for the Zr-rich side (31). So, to corroborate our hypothesis, we carried out a quantitative estimation of the contribution of bulk diffusion to the OSC of ceria and ceria–zirconia mixed oxides by calculating the bulk diffusion coefficients of oxygen from conductivity data. For the calculation of diffusion coefficients, we used the expression (32)

$$D = \frac{f\sigma_i kT}{C_i(Ze)^2}, \qquad [1]$$

where D ($cm^2\ s^{-1}$) is the diffusion coefficient, σ_i ($Ohm^{-1}\ cm^{-1}$) is the ionic contribution to conductivity, k is the Boltzmann constant (JK^{-1}), f is a correlation factor, often called the Haven ratio, whose value for an f.c.c. structure is 0.78146, T is the temperature (K), C_i is the concentration of charge carriers (O atoms $*$ cm^{-3}), and Ze their charge (C). The conductivity was estimated from the experimental values of conductivity and transfer numbers measured recently by Chiodelli *et al.* (33), who reported these data for ceria–zirconia solid solutions in the ceria-rich composition side.

Figure 9 shows that the calculated bulk diffusion coefficient of oxygen ions is approximately two orders of magnitude higher for ceria–zirconia mixed oxides than for pure ceria and that the composition $Ce_xZr_{1-x}O_2$ with $0.5 \le x \le 0.7$ shows the highest values in the temperature range 573–773 K. The values calculated for coefficients are reasonably close to those reported in the literature for quasi-stoichiometric ceria or for ceria-doped solid solutions in the appropriate temperature range. Steele and Floyd give a value of $D = 3.1 \times 10^{-8}\ cm^2\ s^{-1}$ for polycrystalline CeO_2 with an anionic vacancy concentration of less than 0.01% at 1273 K (30). Recently, Kamiya *et al.* found a value of ca. $2 \times 10^{-10}\ cm^2\ s^{-1}$ at a temperature of 1273 K (34). Martin and Duprez measured a value of $D = 5 \times 10^{-18}\ cm^2\ s^{-1}$ for Rh/CeO_2 at 723 K (35), which is lower than our estimate. However, it is worth noting that the measurement of the bulk diffusion coefficient of oxygen ions in ceria and ceria–based catalyst often depends on the concentration of impurities and the texture of samples. Moreover, there is little agreement in the data reported in the literature.

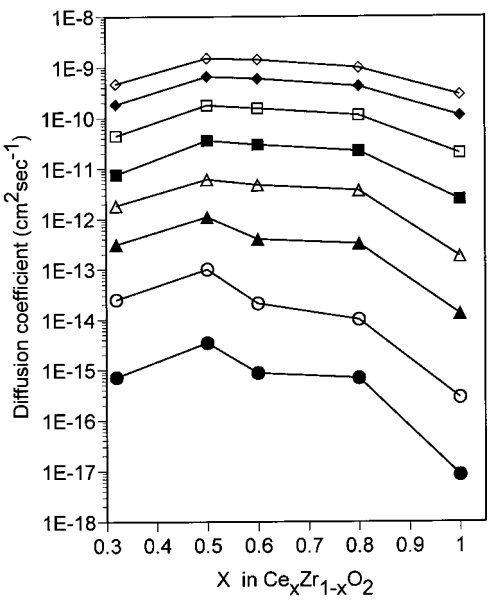

FIG. 9. Calculated diffusion coefficients vs composition at various temperatures: (●) 573 K, (○) 673 K, (▲) 773 K, (△) 873 K, (■) 973 K, (□) 1073 K, (◆) 1173 K, (◇) 1273 K.

Using the above diffusion coefficients, we also estimated the diffusion rate of O^{2-} in ceria and CeO_2–ZrO_2 crystallites using the monodimensional form of the Fick's law of diffusion,

$$N = \frac{D(C_b - C_s)}{L_i}, \qquad [2]$$

where N (molecules $*$ $cm^{-2} * s^{-1}$) is the molecular flux, D ($cm^2 * s^{-1}$) is the diffusion coefficient, C (atoms $*$ cm^{-3}) is the concentration of oxygen ions per unit volume in the bulk (b) and in the surface (s), and L is the characteristic length of the diffusion, i.e., the radius of particles. We assumed that C_b is the bulk concentration of O^{2-} as the particles were fully oxidized (5.04×10^{22} atoms $*$ cm^{-3} for ceria) and C_s is the surface concentration considering a degree of reduction of 1–4%, which is a typical value in our experiments with a time scale of less than 60 s. A radius of particles of ca. 7.8×10^{-7} cm was used for fresh materials, according to recent findings (18). By multiplying the diffusion flux N by the BET surface area ($cm^2 * g^{-1}$), the rate of oxygen migration per gram of catalyst can be obtained and compared with the observed reaction rates (Fig. 10). It appears that, excluding pure ceria, calculated and experimental values are very close, suggesting the possible participation of bulk oxygen in the oxygen storage process. With pure ceria, the time scale of bulk diffusion is too great to be of importance. Calculated rates are remarkably lower than those found experimentally, suggesting that at these temperatures the redox process is confined only to the surface. This is also in agreement with what was found by Nibbelke *et al.* (36), who did not consider bulk oxygen diffusion when modeling CO oxidation under cycling conditions, even for a frequency of 0.25 Hz (i.e., a time scale of 4 s).

Aged Samples

CO oxidation measurements were also carried out on selected samples that had been subjected to redox aging. It is known that one of the most relevant features of ceria–zirconia-based catalysts is their ability to maintain excellent oxygen storage/release properties even when treated at high temperature under reducing conditions. For example,

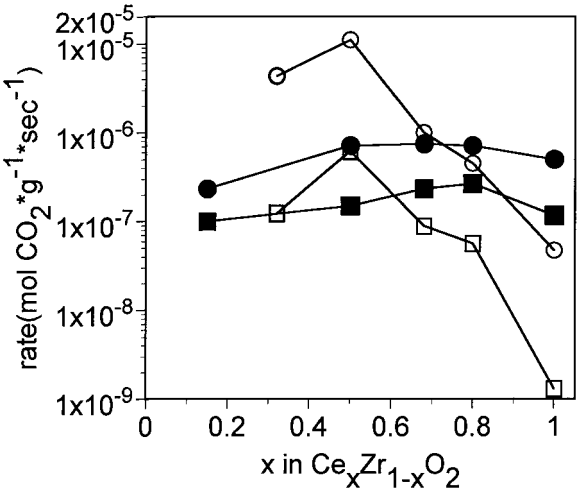

FIG. 10. Comparison between rates of CO_2 production measured under pulse conditions (filled symbols) and those calculated from diffusion data (open symbols). (●, ○) MSA samples, (■, □) LSA samples. For calculating rates a degree of reduction of 1% was assumed.

it has been reported that redox aging often leads to improved reduction behavior at moderate temperature, as measured by temperature-programmed reduction (1).

The aim of these experiments was therefore to ascertain if, and to what extent, CO oxidation activity (in both stationary and cycling modes) is influenced by redox treatments. High-temperature aging treatments were carried out under different conditions for ceria and mixed oxides. The reason for this was to obtain aged catalysts with similar surface area. The results, comparing activity for fresh and aged CeO_2 and $Ce_{0.5}Zr_{0.5}O_2$, are reported in Figs. 11

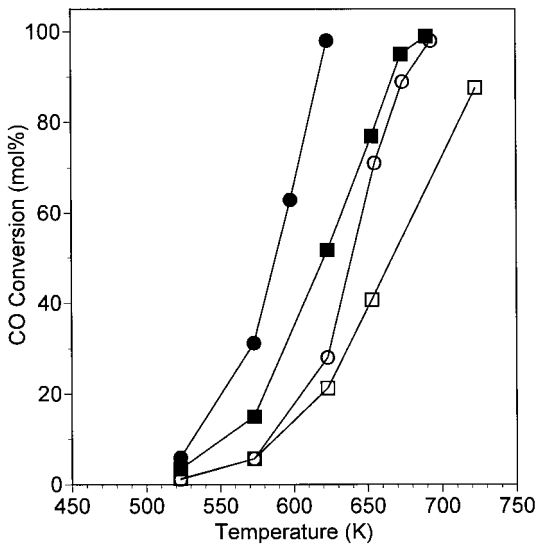

FIG. 11. CO conversion under stationary conditions for fresh (closed symbols) and aged (open symbols) CZ100 (●, ○) and CZ50 (■, □). Reaction conditions: total flow 0.10 N l/min, $P(CO) = 15.2$ Torr, $P(O_2) = 7.6$ Torr, balance He; cat. wt. 80 mg.

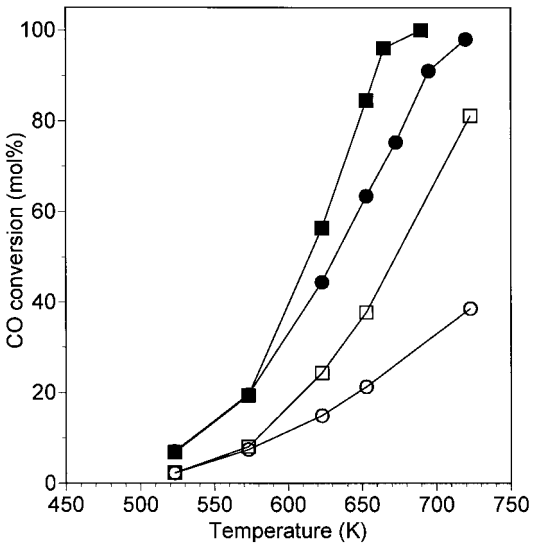

FIG. 12. CO conversion under cycling feedstream conditions for fresh (closed symbols) and aged (open symbols) CZ100 (●, ○) and CZ50 (■, □). Reaction conditions: total flow 0.12 N l/min, cycling frequency ca. 1 Hz, $P(CO) = 30.4$ Torr, $P(O_2) = 15.2$ Torr, balance He, cat. wt. 80 mg.

and 12, while light-off temperatures are summarized in Table 2.

Regardless of the catalysts used, the aging treatment causes an increase in light-off temperatures, which, depending on sample and conditions, span a range of more than 100 K. For CO oxidation under stationary conditions, aging treatment affects ceria and ceria–zirconia in the same way, and the light-off temperature increases by approximately 50 K for both compositions, with pure ceria being more active than ceria–zirconia. This again supports the thesis of an oxidation mechanism which relies on the presence of surface-active sites alone. The drop in surface area produced by aging causes a decrease in the number of active sites, which affects both supports equally.

The introduction of ZrO_2 considerably reduces deactivation after aging if the reaction is carried out in oscillating mode. The light-off temperature of CO oxidation increases from 623 to 773 K with pure ceria, while for the mixed oxides there is an increase of only 60 K. In this range of temperatures, there is no diffusion of vacancies into the bulk of ceria, according to the calculated diffusion rates.

TABLE 2

Comparison between Light-Off Temperatures of Fresh and Aged Materials

	T (50%) steady-state conditions			T (50%) cycling conditions		
Sample	Fresh	Aged	ΔT	Fresh	Aged	ΔT
CZ100	584	635	51	633	756	123
CZ50	615	666	51	617	673	56

The effects of aging at high temperature cause the drop in surface area on both ceria and ceria–zirconia, but the latter, because of the higher mobility of bulk oxygen, suffers a more limited deactivation. With ceria, bulk oxygen is involved only at temperatures higher than 773 K. In the range of temperatures investigated, the exchange of oxygen involves almost exclusively the surface. In this case, aging affects activity dramatically. For solid solution, the bulk oxygen ions are involved at a lower temperature and compensate for the loss of activity due to the drop in surface area.

Higher mobility of bulk oxygen, related to the intrinsic properties of the material, therefore becomes more important for aged samples. In samples of low surface area, the amount of surface oxygen available for exchange is lower and the contribution of bulk oxygen is more significant in the overall redox process.

Other contributions may also be important to explain the higher activity of ceria–zirconia after redox aging conditions. It has been recently reported that structural modifications take place when $Ce_{0.5}Zr_{0.5}O_2$ is subjected to redox aging cycles. Depending on reduction/oxidation temperature, the redox treatments induce the formation of a modified tetragonal fluorite-related structures (5) or even pyrochlore-type phases $CeZrO_4$ (37). While our treatment temperatures were probably not high enough to allow formation of pyrochlore, structural transformation to other fluorite-related phases is likely. These structures are characterized by a displacement of oxygens from their ideal positions, which brings a higher lability of lattice oxygens. This can contribute to a further increase of the overall O^{2-} mobility, thus giving the aged materials an excellent oxygen release ability at low temperatures, even if surface areas are lower than those found in fresh materials.

CONCLUSIONS

In summary, it was shown that oxygen diffusion plays an important role in the enhancement of the redox properties of ceria–zirconia in comparison to ceria, especially if measurements are carried out under dynamic, cycling conditions at relatively low temperatures. This agrees well with other studies, in which the effect of bulk properties of the samples were investigated under different redox environments (3–6, 21, 38).

To see substantial improvements in OSC, the time scale of oxygen ion diffusion into the bulk must be of the same order as the period of one oscillation between a rich and a lean composition. The difference between ceria and ceria–zirconia is highlighted especially at low temperatures (650–750 K) and with longer deviation from the stoichiometric composition. At high temperatures ($T > 850$ K), when oxygen diffusion is faster than the time scale of fluctuation, other factors may become important. The situation remains uncertain in the intermediate temperature range, where, depending on the experimental conditions employed, different contributions can be highlighted (3, 7, 29).

Sintering, which causes an increase in the mean crystallite size, is responsible for deactivation in both ceria and ceria–zirconia. However, the extent of deactivation is much less important in mixed oxides, thanks to the greater availability of bulk oxygen.

ACKNOWLEDGMENTS

We are indebted to Professor Jan Kašpar (Univ. Trieste) for discussion and his comments on the manuscript. Financial support from C.N.R., MURST, and Regione Friuli Venezia Giulia is gratefully acknowledged. The authors thank RHODIA for providing the samples used in this study.

REFERENCES

1. Kašpar, J., Fornasiero, P., and Graziani, M., *Catal. Today* **50**, 285 (1999).
2. Pijolat, M., Prin, M., Soustelle, M., Touret, O., and Nortier, P., *J. Chem. Soc. Faraday Trans.* **91**, 3941 (1995).
3. Fornasiero, P., Di Monte, R., Ranga Rao, G., Kašpar, J., Meriani, S., Trovarelli, A., and Graziani, M., *J. Catal.* **151**, 168 (1995).
4. de Leitenburg, C., Trovarelli, A., Llorca, J., Cavani, F., and Bini, G., *Appl. Catal. A Gen.* **139**, 161 (1996).
5. Fornasiero, P., Balducci, G., Di Monte, R., Kašpar, J., Sergo, V., Gubitosa, G., Ferrero, A., and Graziani, M., *J. Catal.* **164**, 173 (1996).
6. Trovarelli, A., Zamar, F., Llorca, J., de Leitenburg, C., Dolcetti, G., and Kiss, J. T., *J. Catal.* **169**, 490 (1997).
7. Hori, C. E., Permana, H., Ng, K. Y. S., Brenner, A., More, K., Rahmoeller, K. M., and Belton, D., *Appl.Catal. B Environ.* **16**, 105 (1998).
8. Cuif, J. P., Blanchard, G., Touret, O., Seigneurin, A., Marczi, M., and Quéméré, E., SAE Tech. Paper Series 970463, 1, 1997.
9. Jen, H. W., Graham, G. W., Chun, W., McCabe, R. W., Cuif, J. P., Deutsch, S. E., and Touret, O., *Catal. Today* **50**, 309 (1999).
10. Trovarelli, A., *Comm. Inorg. Chem.* **20**, 263 (1999).
11. Rossignol, S., Gerard, F., and Duprez, D., *J. Mater. Chem.* **9**, 1615 (1999).
12. Hashimoto, K., Toukai, N., Hamada, R., and Imamura, S., *Catal. Lett.* **50**, 193 (1998).
13. Overbury, S. H., Huntley, D. R., Mullins, D. R., and Glavee, G. N., *Catal. Lett.* **51**, 133 (1998).
14. Baker, R. T., Bernal, S., Blanco, G., Cordon, A. M., Pintado, J. M., Rodriguez-Izquierdo, J. M., Fally, F., and Perrichon, V., *Chem. Commun.*, 149 (1999).
15. Trovarelli, A., *Catal. Rev. Sci. Eng.* **38**, 439 (1996).
16. Trovarelli, A., de Leitenburg, C., and Dolcetti, G., *CHEMTECH* **27**, 32 (1997).
17. Colón, G., Pijolat, M., Valdivieso, F., Vidal, H., Kaspar, J., Finocchio, E., Daturi, M., Binet, C., Lavalley, J. C., Baker, R. T., and Bernal, S., *J. Chem. Soc. Faraday Trans.* **94**, 3717 (1998).
18. Colon, G., Valdivieso, F., Pijolat, M., Baker, R. T., Calvino, J. J., and Bernal, S., *Catal. Today* **50**, 271 (1999).
19. Kacimi, S., Barbier, J., Taha, R., and Duprez, D., *Catal. Lett.* **22**, 343 (1993).
20. Gonzales-Velasco, J. R., Gutierrez-Ortiz, M. A., Marc, J.-L., Botas, J. A., Gonzales-Marcos, M. P., and Blanchard, G., *Appl. Catal. B Env.* **22**, 167 (1999).
21. Madier, Y., Descorme, C., Le Govic, A. M., and Duprez, D., *J. Phys. Chem. B* **103**, 10999 (1999).

22. Bernal, S., Calvino, J. J., Cifredo, G. A., Gatica, J. M., Perez Omil, J. A., and Pintado, J. M., *J. Chem. Soc. Faraday Trans.* **89**, 3499 (1993).
23. Perrichon, V., Laachir, A., Bergeret, G., Fréty, R., Tournayan, L., and Touret, O., *J. Chem. Soc. Faraday Trans.* **90**, 773 (1994).
24. Conesa, J. C., *Surf. Sci.* **339**, 337 (1995).
25. Sayle, T. X. T., Parker, S. C., and Catlow, C. R. A., *Surf. Sci.* **316**, 329 (1994).
26. Hwang, J. H., and Mason, T. O., *Z. Phys. Chem.* **207**, 21 (1998).
27. Inaba, H., and Tagawa, H., *Solid State Ionics* **83**, 1 (1996).
28. Fornasiero, P., Kašpar, J., and Graziani, M., *Appl. Catal. B Environ.* **22**, L11 (1999).
29. Hori, C. E., Brenner, A., Ng, K. Y. S., Rahmoeller, K. M., and Belton, D., *Catal. Today* **50**, 299 (1999).
30. Steele, B. C. H., and Floyd, J. M., *Proc. Br. Ceram. Trans.* **72**, 55 (1971).
31. Ando, K., Morita, S., and Watanabe, R., *Yogyo-Kyokaishi* **94**, 732 (1986).
32. Tilley, R. J. D., *in* "Principles and Applications of Chemical Defects." Stanley Thornes, Cheltenham, U.K., 1998.
33. Chiodelli, G., Flor, G., and Scagliotti, M., *Solid State Ionics* **91**, 109 (1996).
34. Kamiya, M., Shimada, E., and Ikuma, Y., *J. Ceram. Soc. Jpn.* **106**, 1023 (1998).
35. Martin, D., and Duprez, D., *J. Phys. Chem.* **100**, 9429 (1996).
36. Nibbelke, R. H., Nievergeld, A. J. L., Hoebink, J. H. B. J., and Marin, G. B., *Appl.Catal. B Environ.* **19**, 245 (1998).
37. Omata, T., Kishimoto, H., Otsuka-Yao-Matsuo, S., Ohtori, N., and Umesaki, N., *J. Solid State Chem.* **147**, 573 (1999).
38. Daturi, M., Finocchio, E., Binet, C., Lavalley, J. C., Fally, F., and Perrichon, V., *J. Phys. Chem. B* **103**, 4884 (1999).